GNSS Signal Jamming as Observed from Radio Occultation

Dong L. Wu

Abstract— **The jamming is found to increase significantly in recent years and its impact is evident in GNSS radio occultation (RO) measurements such as those from COSMIC-2. This study presents an algorithm that applies the RO radiometry to detect and monitor long-term variations of GNSS jamming power from a deeply occulted height (H_{SL} = -140 km). At these heights the RO signal amplitude is at its noise level because the GNSS transmitter is far behind the Earth shadow. Thus, any enhanced RO amplitudes from these heights are considered as a jamming signal. The algorithm was successfully applied to two conflict zones: Mediterranean Sea and Middle East (MSME) and Central Africa (CA), where the GPS jamming was frequently used by state-sponsored electronic warfare. The time series of normalized RO amplitude in these regions show a steady increase of the GPS jamming power since 2017, but a sharp decrease since the start of Russo-Ukrainian War.**

Index Terms—**GNSS, Radio Occultation, Jamming, Time Series**

I. INTRODUCTION

Jamming on Global Navigation Satellite System (GNSS) signals poses a great threat to the safety service in civilian air traffic [1-3], regional police and medical emergency operations. It is relatively easy to jam low-power GNSS signals (-160 dBW) and confuse and cause problems for the receivers. Because of the Global Position System (GPS) market expanding from $76B in 2021 to $300B expected for 2029 [4] and the increased military use of GNSS-navigated weapon systems [5-7], the jamming on its receivers continues to be a major issue in GNSS applications. State-sponsored jamming from electronic warfare, especially to GPS signals [8,9], has become common in conflict zones. The International Telecommunication Union (ITU) has issued a warning on potential impacts from the harmful interference and urges the international community to take necessary steps to mitigate the problem [10].

Different from broad L-band radio frequency interference (RFI) seen from space [11,12], the jamming on GNSS receivers is an intentional RFI, often concentrated in a narrow band targeted to a specific transmission frequency such as GPS [13]. These jamming or RFI signals must be flagged and removed in order to produce useful science data in GNSS-reflectometry (GNSS-R) observations [14-17]. Although GNSS-RO is largely based on phase measurements, the RO tracking can be adversely impacted by weak GNSS signals or signal-to-noise ratio (SNR). Because of atmospheric bending and diffraction effects, the RO SNR decreases with limb tangent height and eventually diminishes in a completely occulted situation. To increase the number of RO observations with deep penetration to the lower atmosphere, the RO antennas require a special design with a higher gain than the POD (precise orbit determination) antennas. In the presence of flex power operation from GNSS or jamming from the ground, the number and quality of RO tracking can be significantly impacted.

Detecting jamming from SmallSat/CubeSat has been obtained from the GNSS-POD and GNSS-R measurements. Using the L1 CA signals collected from the POD antennas on LEO satellites, Roberts et al. [16] developed an algorithm that can detect and geo-register RFI using variations in a time series of the SNR measurement. and distinguishable from ionospheric effects. The algorithm is particularly good at fast varying RFI or jamming and produces multi-year global maps of hot spots of these sources. For slowly varying high power sources, the algorithm might have some challenges to distinguish them from other natural variabilities. Furthermore, studying the GNSS-R delay doppler map (DDM) measurement noise, Chew et al. [17] obtained GNSS RFI maps from 2017 to 2022 and found the approximate locations of regional hot spots in the subtropical latitudes over land. The technique can be used to track and evaluate jamming sources at a relatively high revisit rate from an 8-SmallSat constellation.

The objective of this study is to derive a long term GNSS jamming record, using the SNR measurements from RO antennas onboard recent LEO SmallSat/CubeSat constellations [Table 1]. We leverage the RO radiometry algorithm developed for remote sensing of atmospheric water vapor in planetary boundary layer (PBL) [18], to obtain the enhanced RO L1 SNR from very low tangent heights. Multi-satellite records of GNSS jamming are obtained to trace the SNR variability back to 2006 when the COSMIC-1 GNSS-RO constellation was established.

II. GNSS RO OBSERVATIONS

As a limb sounding technique, GNSS-RO can penetrate clouds to profile temperature and water vapor in the lower atmosphere [19,20]. Using the so-called open-loop (OL) operation, the GNSS-RO signal can be tracked far behind the Earth's shadow, sometimes producing a significant signal-to-noise ratio (SNR) at a straight-line height (H_{SL}) between -100 km to -300 km below the surface [21]. Different from closed-loop (CL) operation, in which a phase-locked loop (PLL) circuit is used to track the signal frequency based on previous measurements, in OL operation the receiver relies on a modeled reference signal frequency from orbit dynamics, receiver clock drift, and estimated atmospheric bending effects, to track the

anticipated RO signal regardless of SNR fluctuations. The CL operation works well in the situations where SNR is strong, but a long period of low SNRs would prevent the PLL from updating the reference signal and result in a loss of tracking the GNSS signal.

The introduction of OL operation helps to increase the number of RO soundings because an intermittent loss of tracking often terminates the CL tracking at a low H_{SL}. In addition, the OL observations allow a study of jamming signals from the measurements at these low H_{SL}. As shown in Fig.1, RO profiles are generated from setting/rising limb observations from the radio signal sent by GNSS transmitters. There is little bending at the top of the atmosphere but the dense air in the lower atmosphere can refract the radio wave propagation and cause a bending. As a result, the occulted signal at the receiver on a low-Earth orbit (LEO) is from the transmitter behind Earth's shadow. The bending angle information is used to infer the atmospheric refractivity and derive the temperature/humidity profile. Nowadays, there are a growing number of SmallSat/CubeSat constellations that apply the OL tracking for GNSS-RO observations [Table 1].

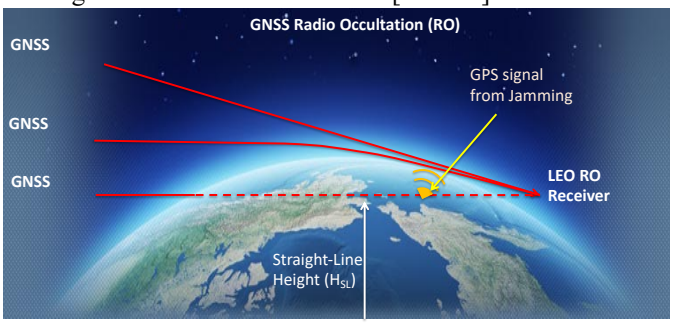


Fig. 1. A schematic of GNSS-RO observations from different straight-line heights (H_{SL}). At a very low H_{SL}, the RO SNR has little signal from GNSS transmitters, and any enhanced SNR or noise is likely from jamming sources at the surface.

TABLE I
SUMMARY OF GNSS-RO OBSERVATIONS

LEO Satellites	Mission lifetime	Init,Final Alt (km)	Lat Coverage	Top RO Ht (km)	Tracked GNSS[5]
CHAMP	2001-2008	450,330	90°S/N	140	G
COSMIC-1[2]	2006-2020	525,810	90°S/N	130	G
MetOp-A	2006-2021	820	90°S/N	90	G
MetOp-B	2012-	820	90°S/N	90	G
MetOp-C	2018-	820	90°S/N	90	G
KOMPSAT-5	2015-	560	90°S/N	135	G
TSX	2009-	520	90°S/N	135	G
TDX	2016-	520	90°S/N	135	G
GRACE	2007-2017	475,300	90°S/N	140	G
COSMIC-2	2019-	715,545	44°S/N	90-130	G, R
PAZ	2018-	520	90°S/N	135	G
S6	2020-	1336	90°S/N	90	G,R
Spire[4]	2018-	varying	90°S/N	170-400	G,R,E,J
GeoOptics	2018-2022	530	90°S/N	130	G, R,E
PlanetIQ	2023-	525, 645	90°S/N	130	G,R,E,C,J

[1] Ascending-orbit equator crossing time (Asc ECT)
[2] The COSMIC1-3 spacecraft never reached the intended orbital altitude and was operated at 725km for the rest of its mission.
[3] The spacecraft started to drift away from the Sun-sync orbit since ~2021.
[4] The Spire constellation acquires RO profiles from GPS, GLONASS, Galileo, and QZSS (briefly before 2021) since 2022.
[5] G, R, E, C, and J are abbreviations respectively for GPS, GLONASS, Galileo, BDS and QZSS.

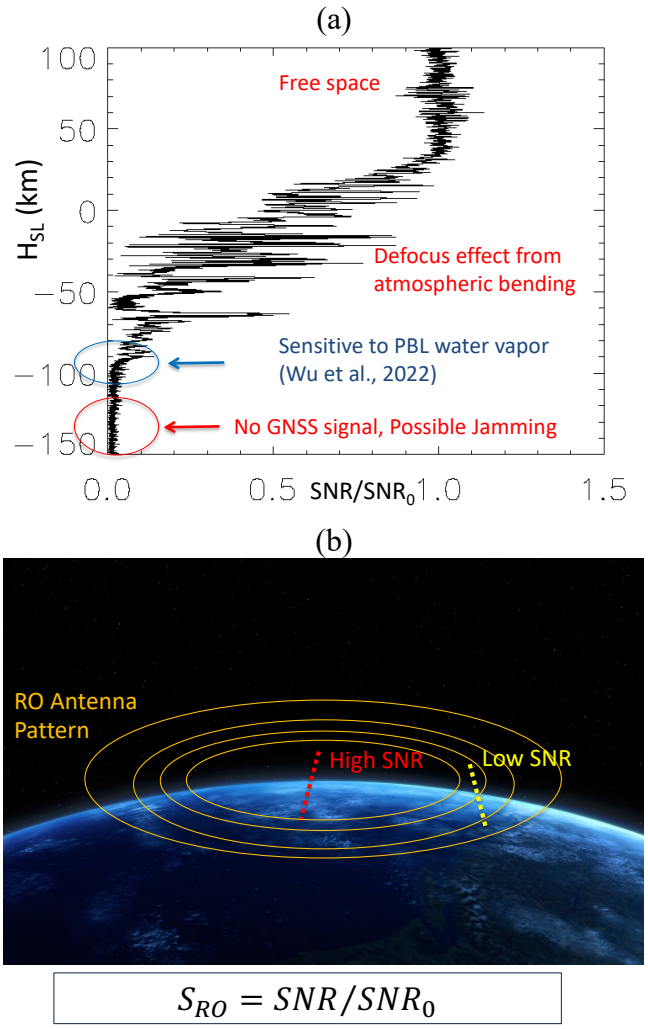


Fig. 2. (a) Typical normalized L1 SNR profile (namely, S_{RO} = SNR/SNR$_0$); (b) Typical RO antenna pattern showing the profiles of high SNR and low SNR measurements.

A typical RO SNR(H_{SL}) profile is shown in Fig.2(a), which is normalized by its free-space value (SNR0) or the mean at H_{SL} > 50 km. The normalization of SNR (S_{RO} = SNR/SNR$_0$) is necessary for the RO radiometry, as the RO amplitude can vary largely from profile to profile. Depending on where the occultation occurs relatively to the angle with respect to the antenna pattern, SNR0 can differ by a factor of 2-4, even when the GNSS transmitter is the same. The normalized SNR can be used to compare the signal powers from different RO receivers

and GNSS transmitters and jamming variations from different periods of time. More details on the S_{RO} algorithm can be found in [18].

III. Jamming on GNSS RO Signals

To identify the jamming power on GNSS signals, we use the S_{RO} values at H_{SL} < -140 km. At this deeply-occulted height, the S_{RO} measurement is close to the receiver noise, because the GNSS transmitter power is mostly blocked by Earth. The contribution from deep refraction by atmospheric water vapor might have some remnants, which diminishes sharply with H_{SL} and is scattered mostly over oceans [18]. Therefore, at low H_{SL}, jamming signals can be detected when they are strong enough above the measurement noise.

To illustrate the significance of jamming signals over the background measurement noise, we map out the S_{RO} averaged at H_{SL} < -140 km for 2019-2022 using all available GPS-RO data from COSMIC-1, Metop, TSX, TDX, KOMPSAT-5, and PAZ. Unfortunately, the COSMIC-1 mission was ending in 2019, and the global RO coverage came mostly from the other satellites. Despite the reduced number of samples in recent years, as shown in Fig.3, jamming signals are clearly seen in the North and Central Africa, the Mediterranean, the Eastern Europe, and the Middle East. The S_{RO} enhancement is spread to Russia in 2022, which is likely related to Russo-Ukrainian War. It is clear that these enhanced S_{RO} values are significantly greater than the atmospheric residuals or other measurement noise seen mostly over oceans.

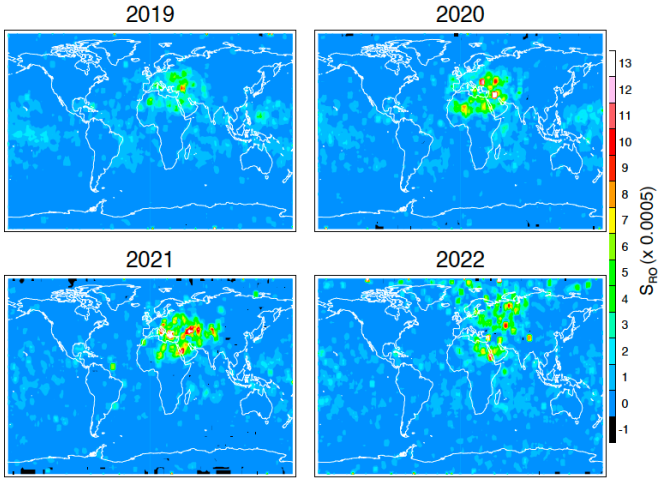


Fig.3. Global maps of annual mean L1 S_{RO} averaged from H_{SL} < -140 km for 2019-2022 using the GPS-tracking RO data acquired by COSMIC-1, Metop-A/B/C, TSX, TDX, KOMPSAT-5, and PAZ.

Fig.4 shows a distribution of enhanced S_{RO} at -140 km in Jan 2022 from COSMIC-2 over the southern Europe and Africa where the hot spot values are significantly above the oceanic background where atmospheric residuals would maximize. The monthly mean S_{RO} are calculated separately for GPS and GLONASS signals, showing that the jamming on GPS signals is much stronger than on GLONASS. Two regions are identified to track their long-term variation of jamming power: Mediterranean Sea and Middle East (MSME) and Central Africa (CA). In 2020, significant jamming on GPS is found over Turkey, Syria, Bulgaria and Somalia, whereas in 2021 strong GPS jamming is evident in Azerbaijan, Turkey, Mediterranean Sea, Tunisia, and South Sudan.

The time series of RO signals from the MSME and CA regions show that the GPS jamming began to increase substantially since 2017 whereas the jamming on GLONASS only had a moderate increase [Fig.5]. The increased jamming on GPS signals seems to be consistent with frequent military uses of GNSS-navigated systems in the regions of conflict. The trends of GPS jamming power variations are also consistent among the measurements from independent GNSS-RO receivers, despite differences in receiver type and LEO altitude. Although the jamming is ubiquitous at all local times in these regions, the daytime power appears to be slightly great than the nighttime.

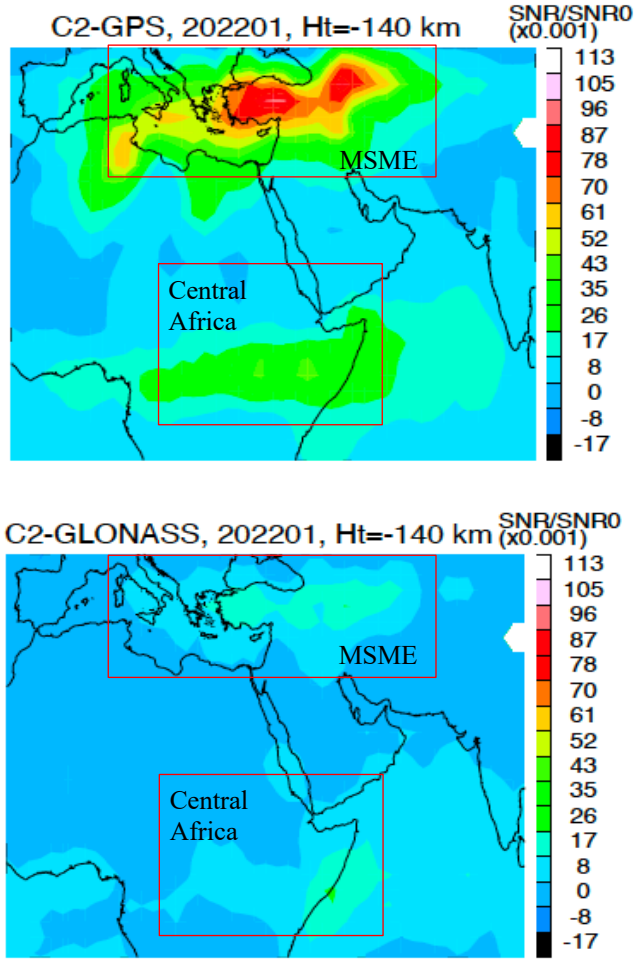


Fig. 4. Distribution of GPS and GLONASS jamming power as observed by COSMIC-2 at H_{SL}=-140 km in Jan 2022, showing hot spots over the Mediterranean Sea and Middle East (MSME) and Central Africa (CA). The two regions are highlighted by the red boxes.

Interestingly, the GPS jamming power shows a sharp decrease in the MSME and CA regions since the start of Russo-Ukrainian War (Feb 2022). The decrease is evident in the COSMIC-2 and MetOp data, although the average S_{RO} jamming power is still above the pre-2017 level. Note that the enhanced S_{RO} in a monthly mean would require a sustained jamming power and often it is from state-sponsored electronic warfare. The socio-political impacts of the Russo-Ukrainian War are complex. Demands for the electrical warfare could shift from one region to the other as conflicts develop, causing changes in a wider region.

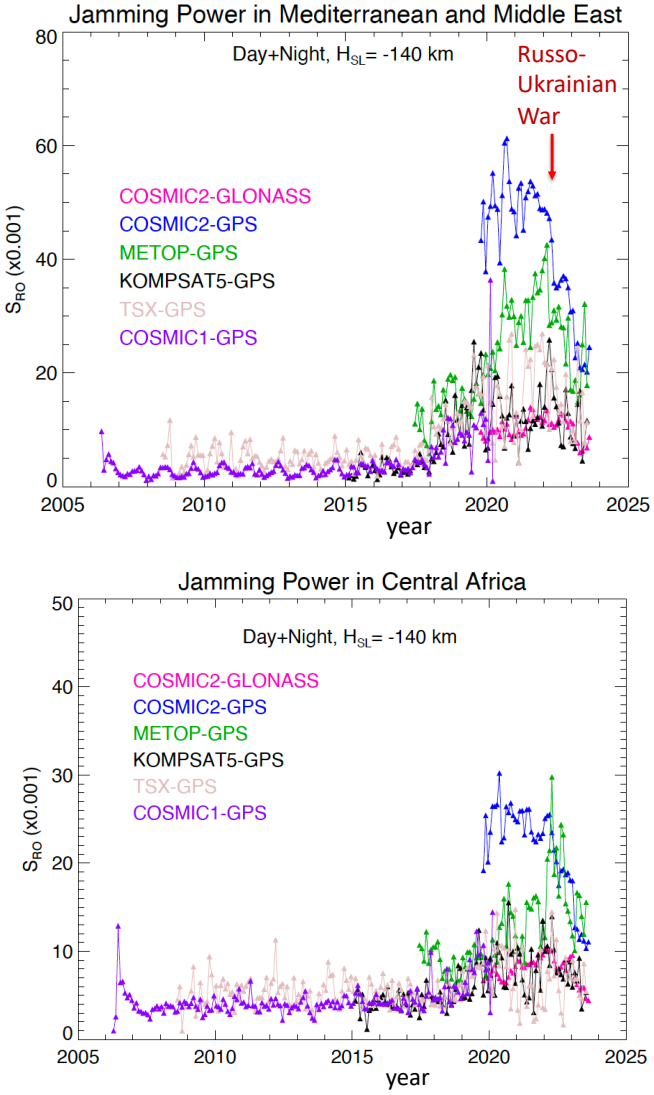


Fig. 5. Time series of the monthly jamming power as observed from different GNSS-RO sensors at deeply-occulted height of -140 km. The earlier period of MetOp-A/B S_{RO} data are excluded in the time series because of the noise data during the open-loop (OL) testing period. The small annual variation in COSMIC-1 S_{RO} before 2017 is likely due to the residuals of the deep refraction from atmospheric water vapor as seen in Fig.3.

IV. Summary

In this study we developed an algorithm to detect and monitor long-term variations of GNSS jamming power, using the normalized GNSS-RO SNR (S_{RO}) measurements from deeply-occulted heights (H_{SL} < -140 km). The algorithm was applied to all GPS-RO L1 SNR observations from COSMIC-1, Metop, TSX, TDX, KOMPSAT-5, and PAZ since 2006. Global distributions of S_{RO} at H_{SL} < -140 km reveal a significant enhancement in the North and Central Africa, the Mediterranean, the Eastern Europe, and the Middle East during 2019-2022. We derived the monthly mean S_{RO} from two conflict zones: Mediterranean Sea and Middle East (MSME) and Central Africa (CA), where the GPS jamming was frequently used by state-sponsored electronic warfare. The time series of these S_{RO} data show that the jamming power started to increase since 2017, but decreased sharply since the Russo-Ukrainian War started. Because of complex socio-political factors, the war's impacts on the GPS jamming in the surrounding regions warrant further investigations.

Acknowledgment

UCAR COSMIC Data Analysis and Archive Center (CDAAC) services for data processing and distribution, and the supports from NASA's Living With a Star (LWS) and Commercial Smallsat Data Acquisition (CSDA) programs are acknowledged.

References

[1] https://safeairspace.net/

[2] https://www.timesofisrael.com/flights-at-ben-gurion-airport-suffer-weeks-of-interruption-to-gps-systems/

[3] https://safety4sea.com/us-marad-gps-interference-incidents-reported-in-the-eastern-mediterranean-sea/

[4] https://www.databridgemarketresearch.com/reports/global-gps-global-positioning-systems-market

[5] https://ops.group/blog/wp-content/uploads/2021/05/opinfo_FAA_Information_Note_-_Turkey_-_PKK_UAS_Attack_-_19_MAY_2021_-_FINAL.pdf

[6] https://www.flyingmag.com/airlines-report-russian-gps-jamming-in-four-regions/

[7] https://eurasiantimes.com/russia-is-jamming-gps-systems-of-powerful-f-22-raptors-f-35-jets-in-middle-east/

[8] Murrian, M.J., Narula, L., Iannucci, P.A., Budzien, S.A., O'Hanlon, B.W., & Humphreys, T.E. (2020). GNSS Interference Monitoring from Low Earth Orbit. arXiv: Signal Processing.

[9] Murrian, M. J., et al. (2021), "First results from three years of GNSS interference monitoring from low Earth orbit," Navigation, Journal of the Institute of Navigation, vol. 68, no. 4, pp. 673–685.

[10] https://www.itu.int/hub/2022/08/warning-harmful-interference-rnss/

[11] P. N. Mohammed, M. Aksoy, J. R. Piepmeier, J. T. Johnson and A. Bringer, "SMAP L-band microwave radiometer: RFI mitigation prelaunch analysis and first year on-orbit observations", IEEE Trans. Geosci. Remote Sens., vol. 54, no. 10, pp. 6035-6047, Oct. 2016.

[12] E. Daganzo-Eusebio, R. Oliva, Yann H. Kerr, S. Nieto, Philippe Richaume, et al. SMOS Radiometer in the 1400-1427-MHz Passive Band: Impact of the RFI Environment and Approach to Its Mitigation and Cancellation. IEEE Trans. Geosci. Remote Sens., 2013, 51 (10), pp.4999-5007.10.1109/TGRS.2013.2259179.ird-00913353

[13] Mitch, Ryan H., Dougherty, Ryan C., Psiaki, Mark L., Powell, Steven P., O'Hanlon, Brady W., Bhatti, Jahshan A., Humphreys, Todd E., "Signal Characteristics of Civil GPS Jammers," Proceedings of the 24th International Technical Meeting of the Satellite Division of The Institute of Navigation (ION GNSS 2011), Portland, OR, September 2011, pp. 1907-1919.

[14] Voosen, Paul, NASA overcomes military's GPS tweaks to peer inside hurricanes. Science, 19 June 2019, doi: 10.1126/science.aay3678

[15] J. Querol, A. Alonso-Arroyo, R. Onrubia, D. Pascual, H. Park and A. Camps, "SNR Degradation in GNSS-R Measurements Under the Effects of Radio-Frequency Interference", IEEE Journal of Selected Topics in Applied Earth Observations and Remote Sensing, vol. 9, no. 10, pp. 4865-4878, Oct. 2016.

[16] T. M. Roberts, T. K. Meehan, J. Y. Tien and L. E. Young, "Detection and localization of terrestrial L-band RFI with GNSS receivers", IEEE Trans. Geosci. Remote Sens., vol. 60, Sep. 2021.

[17] Clara Chew, T. Maximillian Roberts, and Steve Lowe, RFI Mapped by Spaceborne GNSS-R Data. NAVIGATION: Journal of the Institute of Navigation December 2023, 70 (4) navi.618; DOI: https://doi.org/10.33012/navi.618

[18] Wu, D.L.; Gong, J.; Ganeshan, M. GNSS-RO Deep Refraction Signals from Moist Marine Atmospheric Boundary Layer (MABL). Atmosphere 2022, 13, 953. https://doi.org/10.3390/atmos13060953

[19] Melbourne, W. G., Radio Occultations Using Earth Satellites: A Wave Theory Treatment. Jet Propulsion Laboratory California Institute of Technology, Monograph 6, Deep space communications and navigation series, edited by: Yuen, J. H., 610 pp., 2004.

[20] Kursinski, E. R., G. A. Hajj, J. T. Schofield, R. P. Linfield, and K. R. Hardy, 1997: Observing Earth's atmosphere with radio occultation measurements using the global positioning system. J. Geophys. Res., 102, 23 429–23 465, https://doi.org/10.1029/97JD01569.

[21] Sokolovskiy, S., et al., (2014), Observation, analysis, and modeling of deep radio occultation signals: Effects of tropospheric ducts and interfering signals, Radio Sci., 49, 954–970, doi:10.1002/ 2014RS005436.



Dr. Dong L. Wu is the Project Scientist of NASA's Total and Spectral Solar Irradiance Sensor (TSIS) mission at Goddard Space Flight Center (GSFC). His research interests include remote sensing of atmospheric clouds and winds. He was the principal investigator (PI) of Goddard's IceCube project (CubeSat flight demonstration of 883-GHz radiometer for cloud ice measurements). Prior to joining Goddard, Dr. Wu was a Principal Research Scientist and the supervisor of Aerosol and Cloud Group at Jet Propulsion Laboratory (JPL) in California Institute of Technology during 1994-2011. He was a co-investigator Microwave Limb Sounder (MLS) during 1994-2008, CloudSat during 2006-2010, Multi-angle Imaging SpectroRadiometer (MISR) since 2008, and NASA's Global Navigation Satellite Systems (GNSS) since 2007. Dr. Wu received a B.S. degree in space physics from the University of Science and Technology of China in 1985, and M.S. and Ph.D. in atmospheric science from the University of Michigan in 1993 and 1994. He authored and co-authored more than 180 papers on peer-reviewed journals and received a number of awards, including NASA Exceptional Achievement Medal in 2001, 2008 and 2022, JPL Ed Stone award for Outstanding Research Paper in 2006, and Robert H. Goddard Award for Science in 2019.